RESEARCH ARTICLE

Phrenic and intercostal nerves with rhythmic discharge can promote early nerve regeneration after brachial plexus repair in rats

Jing Rui[1, 2], Ya-Li Xu[1], Xin Zhao[1], Ji-Feng Li[2, 3], Yu-Dong Gu[1, 2], Jie Lao[1, 3, *]
1 Department of Hand Surgery, Huashan Hospital, Fudan University, Shanghai, China
2 Key Laboratory of Hand Reconstruction, Ministry of Health, Shanghai, China
3 Shanghai Key Laboratory of Peripheral Nerve and Microsurgery, Shanghai, China

Funding: *This study was supported by the Scientific Research Project of Huashan Hospital of Fudan University of China, No. 2013QD05; the National Natural Science Foundation of China, No. 81501051 & 81572127.*

Graphical Abstract

Rhythmic clusters of discharge in the phrenic and intercostal nerves correlated with nerve regeneration during early stages following brachial plexus repair

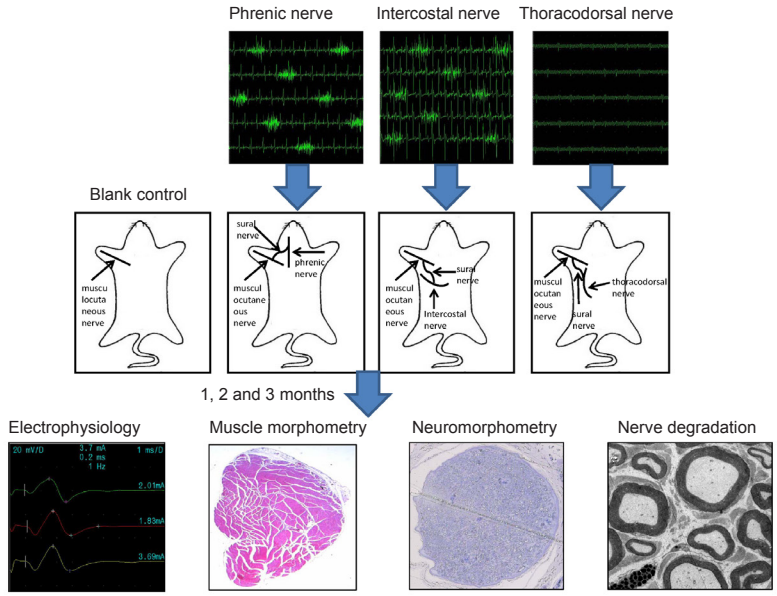

Correspondence to:
Jie Lao, M.D., Ph.D., laojie633@sina.com.

orcid:
0000-0003-4343-6050 (Jie Lao)

doi: *10.4103/1673-5374.232482*

Accepted: *2018-03-28*

Abstract

Exogenous discharge can positively promote nerve repair. We, therefore, hypothesized that endogenous discharges may have similar effects. The phrenic nerve and intercostal nerve, controlled by the respiratory center, can emit regular nerve impulses; therefore these endogenous automatically discharging nerves might promote nerve regeneration. Action potential discharge patterns were examined in the diaphragm, external intercostal and latissimus dorsi muscles of rats. The phrenic and intercostal nerves showed rhythmic clusters of discharge, which were consistent with breathing frequency. From the first to the third intercostal nerves, spontaneous discharge amplitude was gradually increased. There was no obvious rhythmic discharge in the thoracodorsal nerve. Four animal groups were performed in rats as the musculocutaneous nerve cut and repaired was bland control. The other three groups were followed by a side-to-side anastomosis with the phrenic nerve, intercostal nerve and thoracodorsal nerve. Compound muscle action potentials in the biceps muscle innervated by the musculocutaneous nerve were recorded with electrodes. The tetanic forces of ipsilateral and contralateral biceps muscles were detected by a force displacement transducer. Wet muscle weight recovery rate was measured and pathological changes were observed using hematoxylin-eosin staining. The number of nerve fibers was observed using toluidine blue staining and changes in nerve ultrastructure were observed using transmission electron microscopy. The compound muscle action potential amplitude was significantly higher at 1 month after surgery in phrenic and intercostal nerve groups compared with the thoracodorsal nerve and blank control groups. The recovery rate of tetanic tension and wet weight of the right biceps were significantly lower at 2 months after surgery in the phrenic nerve, intercostal nerve, and thoracodorsal nerve groups compared with the negative control group. The number of myelinated axons distal to the coaptation site of the musculocutaneous nerve at 1 month after surgery was significantly higher in phrenic and intercostal nerve groups than in thoracodorsal nerve and negative control groups. These results indicate that endogenous autonomic discharge from phrenic and intercostal nerves can promote nerve regeneration in early stages after brachial plexus injury.

Key Words: *nerve regeneration; endogenous automatic discharge; side-to-side nerve anastomosis; peripheral nerve regeneration; phrenic nerve; intercostal nerve; peripheral nerve injury; neural regeneration*

Introduction

Peripheral nerve regeneration, especially within the brachial plexus, remains challenging in clinical practice. There are several treatments to promote regeneration, including surgery, neurotrophic drugs, recombinant neurotrophic factors, electrical nerve stimulation, and traditional Chinese medicine. Electrical stimulation has been reported to improve axon growth when applied to a nerve anastomosis site (Willand et al., 2015; Badri et al., 2017). Notably, electrical stimulation has been utilized in patients with carpal tunnel syndrome to improve target muscle recovery (Gordon, 2009, 2016; Gordon et al., 2010). Previous studies mainly focused on exogenous electrical stimulation (Gordon, 2009, 2016; Gordon et al., 2010; Willand et al., 2015), but the effects of endogenous discharge, such as from the phrenic and intercostal nerves, remain unclear. Compared to artificial exogenous discharge, endogenous discharge occurs inside the body under physiological conditions, and is continuous. Exogenous discharge can increase nerve repair; therefore, we predict that endogenous discharge, which has similar characteristics to exogenous discharge, may also display such an effect. Therefore, we studied the effects of phrenic and intercostal nerve stimulation on overall nerve regeneration.

The phrenic and intercostal nerves are controlled by the respiratory center and issue rhythmic nerve impulses, causing synchronous contraction and diastolic activity of the diaphragm and intercostal muscles to produce respiratory movement (Kjellgren, 1954; Abdixbir Abra et al., 2016). The phrenic (Gu et al., 1989) and intercostal nerves (Takahashi, 1983) are also widely used as donor nerves for the treatment of brachial plexus avulsion injury. If other nerve transfer combined with phrenic nerve, the results would be positive, which might be due to its endogenous automatic discharge (Rodriguez et al., 2011). However, if we transfer a nerve with

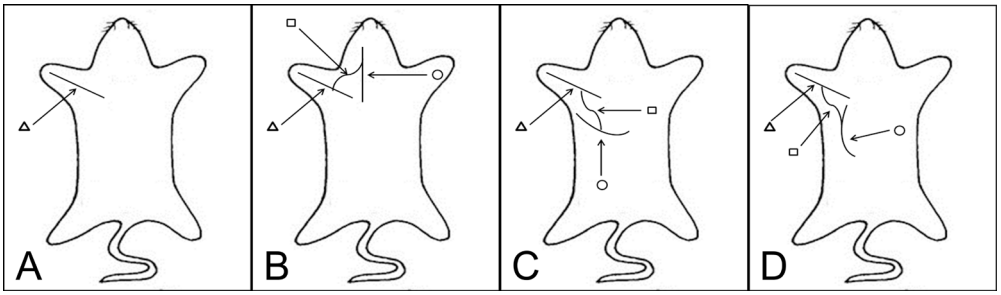

Figure 1 Schematic diagram of nerve autograft establishment.

The musculocutaneous nerve indicated by the triangle was transected first and then directly coapted. The rectangle points to the 2 cm long sural nerve graft one end of which was sutured to the anastomosis site of the musculocutaneous nerve with end-to-side neurorrhaphy, and the other end of which was sutured to the donor nerve, also with end-to-side neurorrhaphy. The circle points to the donor nerve. (A) Negative control group; (B) phrenic nerve group, (C) intercostal nerve group; (D) thoracodorsal nerve group.

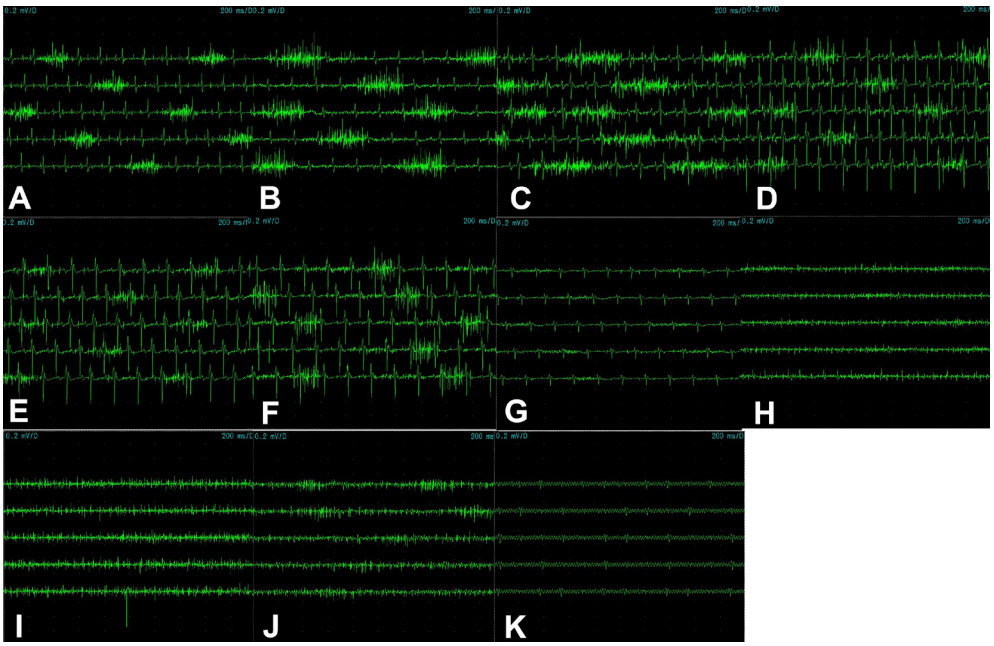

Figure 2 Action potential of the diaphragm (A) in the first to ninth external intercostal muscles from the mid-axillary line (B–J) and latissimus dorsi muscle (K).

The diaphragm showed rhythmic clusters of discharge (A) that was consistent with breathing frequency under anesthesia. The duration of discharge was in line with the duration of inspiration. (B–D) The amplitude from the first to third external intercostal muscles gradually increased. (E–G) However, from the fourth to sixth external intercostal muscles, the amplitude gradually decreased. (H, I) The seventh and eighth external intercostal muscles failed to demonstrate rhythmic clusters of discharges. (J) However, the ninth external intercostal muscle displayed similar rhythmic clusters of discharge but low amplitude. (K) The external intercostal muscles revealed a similar discharge pattern as the diaphragm, which was consistent with breathing frequency under anesthesia. The duration of discharge was in keeping with the duration of inspiration. No independent rhythmic discharges were observed in the latissimus dorsi under anesthesia.

endogenous discharge, the donor nerve function is sacrificed.

According to a previous study (Zheng et al., 2012a), although the clinical efficacy of this phrenic nerve transfer procedure is satisfactory, it can cause impairment of ventilation. To reduce the influence of phrenic nerve transfer on pulmonary function, end-to-side neurorrhaphy was proposed and examined in an animal study. This demonstrated improvements in both recovery of the receptor nerve (Zheng et al., 2012b) and lung function (Wang et al., 2011). This result was supportive of using end-to-side neurorrhaphy to preserve lung function. In this study, we aimed to study the effect of endogenous automatic discharge from the phrenic and intercostal nerves on nerve regeneration recovery after nerve repair.

Materials and Methods

Animals

Eighty-one specific-pathogen-free adult male Sprague-Dawley rats aged about 6 weeks and weighing 200 ± 10 g were purchased from Shanghai Experimental Animal Center of Chinese Academy of Sciences, China (certificate No. SYXK(Hu)2003-0033). Nine rats were randomly assigned to a diaphragm group, an intercostal muscle group and a latissimus dorsi muscle group. These groups were used for discharge pattern detection. The remaining 72 rats were randomly divided into: negative control (n = 18) (**Figure 1A**), phrenic nerve (n = 18) (**Figure 1B**), intercostal nerve (n = 18) (**Figure 1C**), and thoracodorsal nerve groups (n = 18) (negative control) (**Figure 1D**). In each group, the rats were further randomized into three sub-groups for measurements at 1, 2 and 3 months after surgery.

The rats were anesthetized intraperitoneally with pentobarbital sodium (50 mg/kg; Shanghai Reagent Company, Shanghai, China). All surgery and experimental procedures were performed in accordance with the Animal Ethics Committee of Fudan University, China (approval No. 20171631A574). All surgical procedures were conducted under a surgical microscope at 10× magnification. The right side was taken as the surgical side.

Nerve discharge pattern detection

A Keypoint 4 channel electrophysiological apparatus (Dantes, Skovlunde, Denmark) was used for collecting action potentials, discharge patterns, amplitudes, and frequencies.

For the diaphragm group, an arc incision was made under the costal margin. A recording electrode (manufactured in-house) wrapped in insulation material with a 5 mm tip exposed was inserted 15° horizontally into the diaphragm. A stable action potential signal was acquired for 1 minute at eupnea.

For the intercostal muscle group, the recording electrode was inserted into the external intercostal muscle to record the action potentials of the first to the ninth external intercostal muscles.

For the latissimus dorsi muscle group, the recording electrode was inserted into the latissimus dorsi muscle.

Nerve transfer procedure

For the negative control group, the brachial plexus bundle branches were exposed in the subclavian area. The musculocutaneous nerve was identified at the terminal point into the biceps. The muscular branch was proximally exposed for 10 mm, and then transected at the middle point of the initial site and the inserting site to the biceps (Wang et al., 2011). Then, the two nerve ends were directly coated with 12-0 Prolene sutures tension-free (**Figure 1A**). The skin was closed using an interrupted 5/0 silk suture.

The phrenic nerve group, intercostal nerve group and thoracodorsal nerve group underwent the same procedure as the negative control group. In addition, 2 cm of the sural nerve was isolated from the left leg of the same rat. One end of the graft was sutured to the anastomosis site of the musculocutaneous nerve with end-to-side neurorrhaphy, and the other end of the graft was sutured to the side of the phrenic nerve (phrenic nerve group), the third external intercostal nerve (intercostal nerve group) or the thoracodorsal nerve (thoracodorsal nerve group) by end-to-side neurorrhaphy at the level of the C_6 nerve root using 12-0 Prolene (**Figure 1**). The epineurium of the phrenic nerve was removed; however, the perineurium was kept at the site of coaptation (Wang et al., 2011).

The animal model was successfully established in all 72 rats and the surgical procedure was well tolerated. All rats survived during experiments and no surgery-related complications or deaths occurred within three months after surgery. No functional decline, with the exception of elbow flexion, was observed after surgery.

Evaluation of receptor nerve recovery

At 1, 2 and 3 months post-surgery, six rats from each group were randomly selected and underwent functional tests, including nerve conductance studies and muscle tetanic contraction force testing. Muscle weight was measured and histological examination of nerves and number of nerve fibers were also examined under light and electron microscopy (Wang et al., 2011, 2014; Rui et al., 2012).

Nerve conduction study

An electrical stimulus by a Keypoint 4 channel electrophysiological apparatus with a single square wave shock (2.0 mA super pulse current, 0.2 ms pulse width, 1 Hz stimulus frequency) was used distally to the coaptation site of the musculocutaneous nerve. The maximum amplitude of compound muscle action potential (CMAP) was recorded from the biceps using a concentric needle-recording electrode inserted vertically into the muscle. Experiments were performed at 25°C and the muscle and nerves were kept moist with warm normal saline.

Muscle tetanic contraction force test

The tetanic forces of both the ipsilateral and contralateral biceps muscles were detected by a force displacement transducer (JZJ101, Chengdu Instrument, Chengdu, China) connected to a RM6240BD multichannel physiology signal collection system. The negative side (left side) was tested first. The distal portion of the biceps brachii muscle was severed at the attachment point and dissected proximally to its origin. Next, the distal stump that had been tied with a silk suture was attached to the tension transducer. After the biceps was adjusted to an optimal initial length, a train of electric stimulation at 5

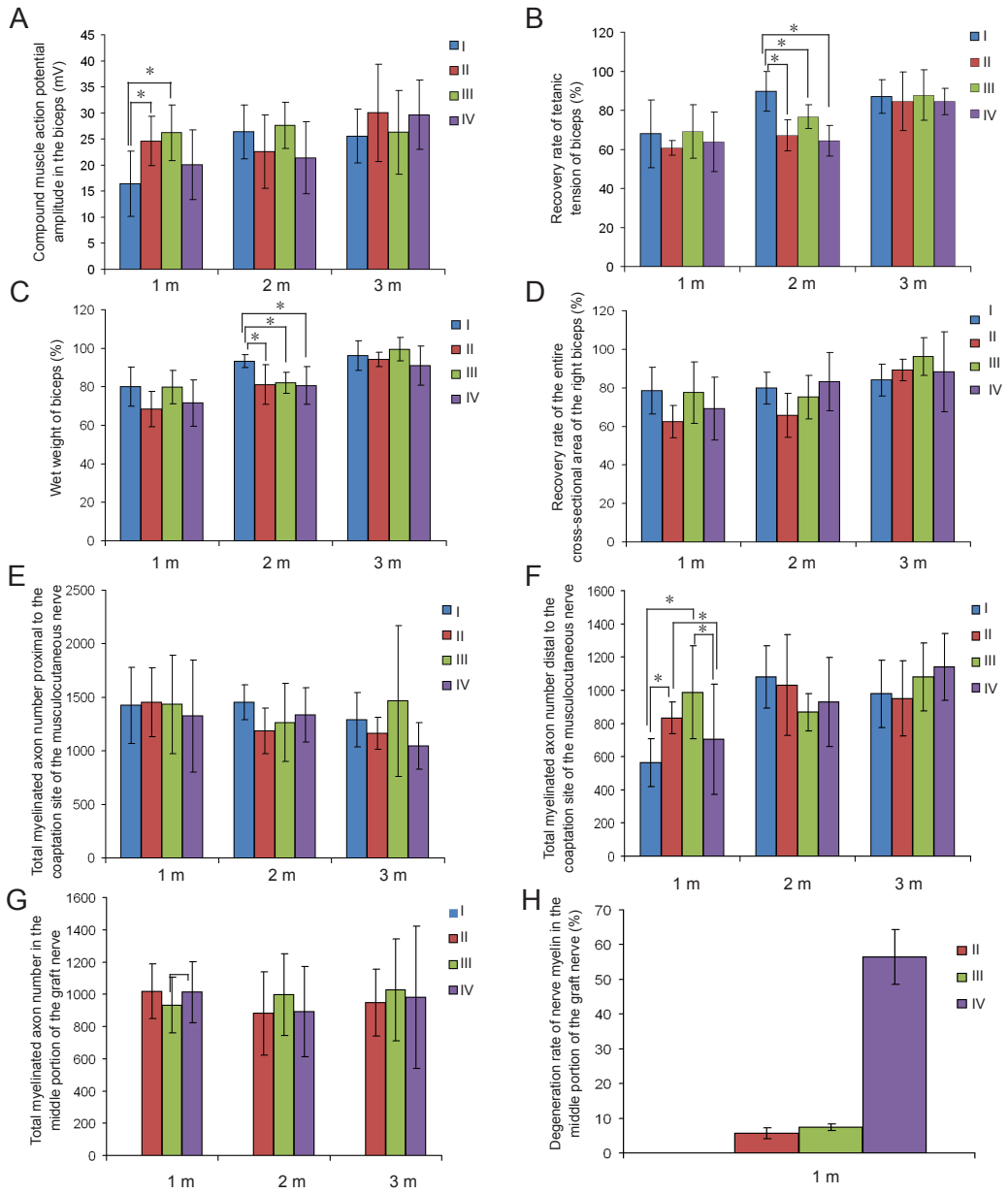

Figure 3 Nerve regeneration evaluation at 1, 2 and 3 months post-surgery among all groups.

Compound muscle action potential amplitude in the biceps (A), the recovery rate of tetanic tension and wet weight of biceps (B, C), the recovery rate of the entire cross-sectional area of the right biceps (D), total myelinated axon number proximal to the coaptation site of the musculocutaneous nerve (E), total myelinated axon number distal to the coaptation site of the musculocutaneous nerve (F), total myelinated axon number in the middle portion of the graft nerve (G), and the degeneration rate of nerve myelin in the middle portion of the graft nerve (H) are presented in the graphs. Data are shown in the mean ± SD (one-way analysis of variance followed by Student-Newman-Keuls *post hoc* test). ∗$P < 0.05$. I: Negative control group; II: phrenic nerve group; III: intercostal nerve group; IV: thoracodorsal nerve group. m: Month(s).

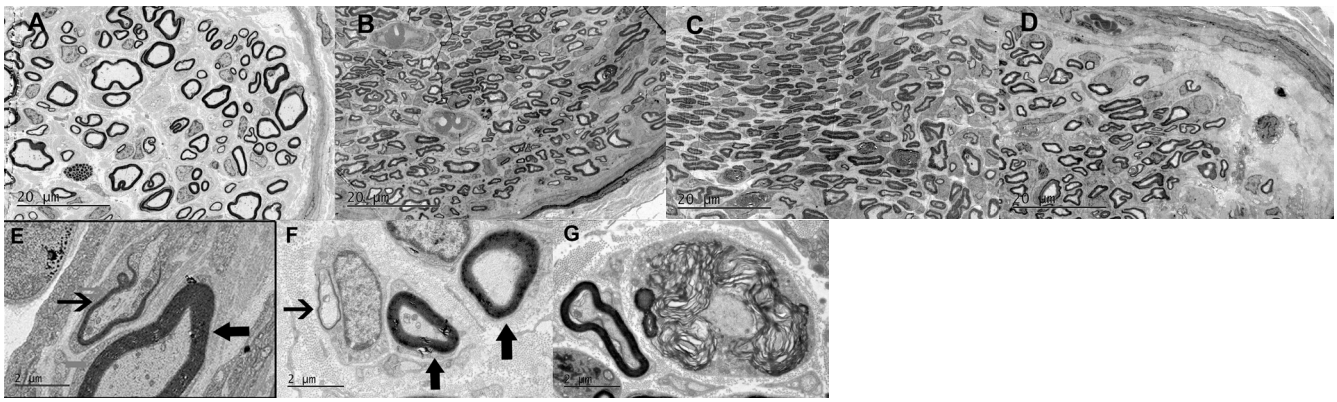

Figure 4 Scanning electron microscopy of nerve axon regeneration.

Original magnification: 1850× in A–D. A greater number of higher density myelinated axons could be detected distal to the coaptation site of the musculocutaneous nerve in the phrenic nerve group and intercostal nerve group compared with that in the negative control group and thoracodorsal nerve group at 1 month post-operation. Original magnification: 13,500× in E–G. In the thoracodorsal nerve group (G), a large amount of the myelin started to degenerate and the normal structure disappeared, leaving fragments that look like floccus, and that could be detected in the middle portion of the graft nerve; while in the phrenic nerve group (E) and intercostal nerve group (F), the axons showed improved morphology and small amounts of degenerated myelin. The thin arrows point to newly formed axons, while the thick arrows point to mature axons.

V amplitude, 100 Hz frequency, and 0.1 ms wave width was placed on the surface of the muscle with two hooked AgCl stimulating electrodes to detect the peak amplitudes of tetanic muscle contractions. Data were recorded with an oscillograph. The muscle tetanic tension recovery rate is expressed as a percentage of that obtained on the contralateral side.

Muscle weight

Biceps muscles were detached from the bone at their origin and terminal point, and then weighed immediately to prevent tissue desiccation with an electronic scale (R200D, 0.0001 precision, Sartorius, Houston, TX, USA). The wet muscle weight is expressed as a percentage relative to that of the control group. The wet muscle weight recovery rate is expressed as a percentage of that on the contralateral side.

Hematoxylin and eosin staining

The harvested biceps were fixed with 10% formalin, and then dehydrated in serial concentrations of alcohol and embedded with olefin. Five-micron thick sections from the middle of the muscles were cut, and then stained with hematoxylin and eosin. Digital image analysis software i-solution (IMT i-Solution Inc., Vancouver, BC, Canada) was employed to measure and calculate the entire cross-sectional area at a 50× magnification. The entire cross-sectional area recovery rate is expressed as a percentage of that from the contralateral side.

Toluidine blue staining

The musculocutaneous nerve segment from the origin to 1 cm distal to the coaptation site was used to measure the number of nerve fibers. The specimens were fixed with 0.1 M glutaraldehyde for 4 hours (pH 7.4, 4°C) and post-fixed with 2% osmium tetroxide for 2 hours, and then dehydrated in serial concentrations of alcohol and embedded in Epon. Sections 0.5 μm thick were cut at 3 mm proximal to the coaptation site (labeled as proximal to coaptation site), and at 8 mm distal to the coaptation site (labeled as distal to coaptation site) of the nerve segment. Slices were stained with 5% toluidine blue, and observed with a light microscope at 200× magnification (LeicaDWLB2, Leica, Wetzlar, Germany). Five images were randomly taken from each sample using a DC300F color digital camera (Leica) and were analyzed by i-solution software (IMT i-Solution Inc Vancouver, BC, Canada). The total myelinated axon number was obtained by measuring the area of view and myelinated axon counts, as well as calculating the mean density of myelinated axons.

Observation of nerves by electron microscopy

Three samples from each group were observed at one month post-operation by electron microscopy for nerve ultra-micro-structure changes. The specimens were fixed with 2.5% glutaraldehyde and post-fixed with 1% osmium tetroxide. The nerve samples were then dehydrated in serial concentrations of alcohol and embedded in Epon 812. Cross-sections were cut on a microtome (LKB-I, Microtome, Bromma, Sweden), and then stained with 3% uranyl acetate and lead citrate. The slices were observed using a transmission electron microscope (Philips, CM-120, Amsterdam, The Netherlands). The myelinated axon number in the middle portion of the graft nerve (1 cm from the coaptation site) was counted. The myelinated axon in the middle portion of the graft nerve was observed. Three images were randomly taken from each sample. The degeneration rate of nerve myelin is expressed as the percentage of the degenerated myelin axon number to the total myelinated axon number.

Statistical analysis

All statistical analyses were performed by Prism 5.0 (Graphpad, La Jolla, CA, USA). Data are presented as the mean ± SD. One-way analysis of variance followed by Student-Newman-Keuls *post hoc* tests were used to analyze multiple comparisons in data with normal distributions and homogeneous variances. A value of $P < 0.05$ was considered statistically significant.

Results

Action potentials of the diaphragm, external intercostal muscles and latissimus dorsi muscle

The diaphragm showed rhythmic clusters of discharge (**Figure 2A**) with a maximum amplitude of 0.3–0.4 mV and the interval between two discharges was 1.0–1.2 seconds, which was consistent with breathing frequency under anesthesia. The duration of discharge was 0.2–0.3 seconds, in line with the duration of inspiration.

In addition, the external intercostal muscles showed rhythmic clusters of discharge observed from the mid-axillary line. The amplitude from first to third external intercostal muscles gradually increased (**Figure 2B–D**), and the maximum amplitude was 0.3–0.4 mV. However, from the fourth to sixth external intercostal muscles, the amplitude gradually decreased (**Figure 2E**), with the maximum amplitude approximately 0.1 mV (**Figure 2F, G**). The seventh and eighth external intercostal muscles failed to demonstrate rhythmic clusters of discharges (**Figure 2H, I**). However, the ninth external intercostal muscle displayed similar rhythmic clusters of discharge but low amplitude (**Figure 2J**). The external intercostal muscles revealed a similar discharge pattern as the diaphragm with a 1-second interval between two discharges, which was consistent with breathing frequency under anesthesia. The duration of discharge was approximately 0.2–0.3 seconds, in keeping with the duration of inspiration. No independent rhythmic discharges were observed in the latissimus dorsi under anesthesia (**Figure 2K**).

Receptor nerve function recovery in the nerve autograft animal model

The CMAP was recorded from the biceps at 1, 2 and 3 months post-operation when stimulating the musculocutaneous nerve. CMAP amplitude was significantly higher at 1 month after surgery in phrenic and intercostal nerve groups compared with the thoracodorsal nerve and negative control groups ($P = 0.046$). However, no significant difference was found between 2 and 3 months after surgery in each group ($P = 0.181, 0.795$; **Figure 3A**).

We next examined the recovery rate of tetanic tension (**Figure 3B**) and wet weight of the right biceps (**Figure 3C**). The recovery rate of tetanic tension and wet weight of the right biceps were significantly lower at 2 months after surgery in the phrenic nerve, intercostal nerve, and thoracodorsal nerve groups compared with the negative control group

(P = 0.002 for tetanic tension, P = 0.042 for wet weight). However, there were no differences at 1 and 3 months after surgery (P = 0.687, 0.939 for tetanic tension, P = 0.108, 0.082 for wet weight).

The recovery rate of the entire cross-sectional area of the right biceps did not show any differences at 1, 2, or 3 months after surgery (P = 0.160, 0.163, 0.311; **Figure 3D**).

Receptor nerve structural recovery in the nerve autograft animal model

The total myelinated axon number of the musculocutaneous nerve proximal to the coaptation site (P = 0.891, 0.241, 0.467; **Figure 3E**), and in the middle portion of the graft nerve (P = 0.440, 0.824, 0.875; **Figure 3G**) did not reveal any significant differences between groups. However, total myelinated axon number in the musculocutaneous nerve distal to the coaptation site at 1 month after surgery in phrenic and intercostal nerve groups was significantly higher than those in thoracodorsal nerve and negative control groups (P = 0.007; **Figure 3F**). No significant difference was found at 1 to 3 months post-operation among all the groups (P = 0.316, 0.458).

Using electron microscopy, we observed regenerated axons with a large diameter and areas of myelination proximal to the coaptation site of the musculocutaneous nerve in all four groups at 1 month post-operation, as well as newly formed and mature axons at a higher magnification. However, distal to the coaptation site of the musculocutaneous nerve (**Figure 4 A–D**), a higher density of myelinated axons was shown in the phrenic nerve and intercostal nerve groups compared with the thoracodorsal nerve and the negative control groups. In the medial portion of the graft nerve (**Figures 3H**, **4E–G**), the degeneration rate in the phrenic nerve and intercostal nerve groups was significantly lower than in the negative control group (P = 0.001).

Discussion

Compared with the control groups, the phrenic and intercostal nerve groups, which have endogenous automatic discharge, showed higher CMAP amplitude, higher total myelinated axon number distal to the coaptation site of the musculocutaneous nerve and lower degeneration rates in the medial portion of the graft nerve at early stages. We assessed multiple aspects of nerve regeneration, including axonal sprouting, growth, and reinnervation of the appropriate target cells. Electrophysiology was used to evaluate nerve recovery by stimulating the nerve and inducing muscle contraction, which was reflected by the potential and amplitude of CMAP. The structural nerve recovery, as assessed by axon number and muscle cross-sectional area, was examined by histology. The muscle tetanic contraction force test and muscle moist weight were used to evaluate functional recovery. As demonstrated by previous studies, according to the chronological order of nerve regeneration, axon number is the first indicator of recovery, followed by electrophysiology, muscle moist weigh, muscle cross-sectional area, muscle tetanic contraction force and behavioral responses (Nichols et al., 2005; Manoli et al., 2014). Our results matched this chronological order of nerve regeneration. A decline in elbow flexion was observed in this study, due to the radial nerve that innervated the brachioradialis; therefore, functional tests such as grooming were inappropriate for this study. We used 1, 2 and 3 month post-operation time points to study nerve recovery because of the short distance from the musculocutaneous nerve to the biceps, leading to a short regeneration time. At 3 months post-operation, recovery in all groups had plateaued.

CMAP and myelinated axon counts are indicators of early stages of nerve regeneration. The area under CMAP amplitude and the waveform associated with myelinated axon count were used to reflect the status of motor nerve regeneration (Vleggeert-Lankamp et al., 2004; Schulz et al., 2014). In our study, these two early indicators showed that the phrenic and intercostal nerves promote receptor nerve regeneration after early stage side-to-side nerve anastomosis. The degeneration rate of nerve myelin in the middle portion of the graft nerve in phrenic and intercostal groups also indicated that nerve degeneration was low in collateral sprouting and axon regeneration, which may be the mechanism of endogenous automatic nervous discharge to promote nerve repair. After two months, tetanic tension and wet muscle weight in phrenic and intercostal groups were inhibited compared with the negative control group, suggesting that nerve regeneration may be blocked by scar compression due to the three nerve ends (the proximal and distal ends of the musculocutaneous nerve and the graft nerve) sutured together. In later stages, there were no significant differences among groups, which was consistent with Mackinnon's finding that a "blow-through" effect is apparent in inter-groups in small animal models (Brenner et al., 2008; Banks et al., 2015). This study also showed that during eupnea, both the phrenic and intercostal nerves had rhythmic clusters of discharge. We found that discharge intensity decreased from upper ribs to lower ribs, which may correlate with anatomical positioning and function. During inhalation, the upper external intercostal muscles drive more ribs than the lower muscles, thus a larger force is required for upper external intercostal muscles, which may have a higher intensity discharge of the intercostal nerves. Therefore, we used the upper intercostal nerves for our study. We observed that the ninth external intercostal muscle displayed rhythmic clusters of discharge from the mid-axillary line because it was affected by the rhythmic discharge of the neighboring diaphragm.

We chose rats as an animal model, because the brachial plexus structure of rats is highly similar to that in humans (Bobkiewicz et al., 2017). The short distance from the musculocutaneous nerve to the target muscle helped avoid interference from muscle atrophy. The musculocutaneous nerve in the subclavian area is close to the phrenic nerve, intercostal nerve and thoracodorsal nerve, which was convenient for manipulation. In addition, biceps were easily harvested for further testing. The musculocutaneous nerve anastomosed after cutting was taken as a control, which was similar to the simple nerve repair procedure currently performed clinically. The thoracic dorsal nerve, which has myotonia and an arrhythmic discharge pattern, was used as a negative control, and was compared with the phrenic and intercostal nerves, which have automatic and continuous discharge. Thus, we developed a novel animal model with endogenous automatic discharge and normal nerve repair after injury.

End-to-side neurorrhaphy was first reported by Kennedy (1900). Recently, many studies suggested that collateral sprouting through the epineurium and perineurium can regenerate nerves, and the lateral window makes regeneration much easier. In this study, side-to-side neurorrhaphy with nerve autograft and a lateral window in the epineurium was conducted to promote nerve regeneration, thereby avoiding a decline in respiratory function. This animal had the advantage of endogenous automatic discharge from the phrenic and intercostal nerves on nerve regeneration and also preservation of lung function. Although the phrenic and intercostal nerve groups showed good results only at the early stages, it still has clinical potential to avoid muscle atrophy because it benefits from an early recovery effect, and saves time for nerve regeneration especially for old nerve injury. Therefore, using a side-to-side approach by adding phrenic and intercostal nerves to traditional nerve repair procedures may be clinically promising.

Phrenic and intercostal nerves showed rhythmic clusters of discharge, which was consistent with breathing frequency, while the thoracodorsal nerve showed no similar effects. In addition, our results indicate that the phrenic and intercostal nerve scans stimulate nerve regeneration by a positive effect on nerve receptors at the early stage, a negative effect in the middle stages, and no effect at the late stage. These results may provide a potential target for further clinical studies. Moreover, we will combine the endogenous stimulation described here with other factors known to improve repair, such as neurotrophic drugs, recombinant neurotrophic factors, and traditional Chinese medicine in our future study.

Acknowledgments: *We are thankful to our colleagues Dr. Xu, Dr. Gao, and Dr. Guan who have generously offered their assistance with this work.*
Author contributions: *JL participated in study design, data analysis, trouble shooting, paper editing and paper review. JR was in charge of animal experiment, literature search, data acquisition, data analysis, statistical analysis, and paper preparation. YLX was responsible for nerve discharge pattern detection. JFL participated in nerve histological studies. XZ was in charge of trouble shooting. YDG was responsible for study design and trouble shooting. All authors approved the final version of the paper.*
Conflicts of interest: *No potential conflict of interest was reported by the authors.*
Financial support: *This study was supported by the Scientific Research Project of Huashan Hospital of Fudan University of China, No. 2013QD05; the Natural Science Foundation of China, No. 81501051, 81572127. The funding sources played no role in study design, data collect, data analysis, data interpretation or writing of the paper.*
Institutional review board statement: *All surgery and experimental procedures were performed in accordance with the Animal Ethics Committee of Fudan University of China (approval No. 20171631A574). The experimental procedure followed the National Institutes of Health Guide for the Care and Use of Laboratory Animals (NIH Publications No. 8023, revised 1985).*
Copyright license agreement: *The Copyright License Agreement has been signed by all authors before publication.*
Data sharing statement: *Datasets analyzed during the current study are available from the corresponding author on reasonable request.*
Plagiarism check: *Checked twice by iThenticate.*
Peer review: *Externally peer reviewed.*

Open peer reviewer: *Xue Deng, University of Hong Kong, China.*

References

Abdixbir Abra, Li P, Ilhamjan Usman, Exmetjan Yüsup (2016) Phrenic nerve transfer versus intercostal nerve transfer for the repair of brachial plexus root avulsion injuries. Zhongguo Zuzhi Gongcheng Yanjiu 20:7660-7665.

Badri O, Shahabi P, Abdolalizadeh J, Alipour MR, Veladi H, Farhoudi M, Zak MS (2017) Combination therapy using evening primrose oil and electrical stimulation to improve nerve function following a crush injury of sciatic nerve in male rats. Neural Regen Res 12:458-463.

Banks CA, Knox C, Hunter DA, Mackinnon SE, Hohman MH, Hadlock TA (2015) Long-term functional recovery after facial nerve transection and repair in the rat. J Reconstr Microsurg 31:210-216.

Bobkiewicz A, Cwykiel J, Siemionow M (2017) Anatomic variations of brachial and lumbosacral plexus models in different rat strains. Microsurgery 37:327-333.

Brenner MJ, Moradzadeh A, Myckatyn TM, Tung TH, Mendez AB, Hunter DA, Mackinnon SE (2008) Role of timing in assessment of nerve regeneration. Microsurgery 28:265-272.

Gordon T (2009) The role of neurotrophic factors in nerve regeneration. Neurosurg Focus 26:E3.

Gordon T (2016) Electrical stimulation to enhance axon regeneration after peripheral nerve injuries in animal models and humans. Neurotherapeutics 13:295-310.

Gordon T, Amirjani N, Edwards DC, Chan KM (2010) Brief post-surgical electrical stimulation accelerates axon regeneration and muscle reinnervation without affecting the functional measures in carpal tunnel syndrome patients. Exp Neurol 223:192-202.

Gu YD, Wu MM, Zhen YL, Zhao JA, Zhang GM, Chen DS, Yan JG, Cheng XM (1989) Phrenic nerve transfer for brachial plexus motor neurotization. Microsurgery 10:287-289.

Kennedy R (1900) On the restoration of co-ordinated movements after nerve crossing, with interchange of function of the cerebral cortical centres. [Abstract]. Proc R Soc Lond 67:431-435.

Kjellgren K (1954) The innervation of the biliary system and the proximal part of the duodenum from a surgical aspect. Acta Chir Scand 107:230-243.

Manoli T, Werdin F, Gruessinger H, Sinis N, Schiefer JL, Jaminet P, Geuna S, Schaller HE (2014) Correlation analysis of histomorphometry and motor neurography in the median nerve rat model. Eplasty 14:e17.

Nichols CM, Myckatyn TM, Rickman SR, Fox IK, Hadlock T, Mackinnon SE (2005) Choosing the correct functional assay: a comprehensive assessment of functional tests in the rat. Behav Brain Res 163:143-158.

Rodriguez A, Chuang DC, Chen KT, Chen RF, Lyu RK, Ko YS (2011) Comparative study of single-, double-, and triple-nerve transfer to a common target: experimental study of rat brachial plexus. Plast Reconstr Surg 127:1155-1162.

Rui J, Dadsetan M, Runge MB, Spinner RJ, Yaszemski MJ, Windebank AJ, Wang H (2012) Controlled release of vascular endothelial growth factor using poly-lactic-co-glycolic acid microspheres: in vitro characterization and application in polycaprolactone fumarate nerve conduits. Acta Biomater 8:511-518.

Schulz A, Walther C, Morrison H, Bauer R (2014) In vivo electrophysiological measurements on mouse sciatic nerves. J Vis Exp.

Takahashi M (1983) Studies on conversion of motor function in intercostal nerves crossing for complete brachial plexus injuries of root avulsion type. Nihon Seikeigeka Gakkai Zasshi 57:1799-1807.

Vleggeert-Lankamp CL, van den Berg RJ, Feirabend HK, Lakke EA, Malessy MJ, Thomeer RT (2004) Electrophysiology and morphometry of the Aalpha- and Abeta-fiber populations in the normal and regenerating rat sciatic nerve. Exp Neurol 187:337-349.

Wang L, Jiang Y, Lao J, Zhao X (2014) Contralateral C7 transfer to lower trunk via the prespinal route in the repair of brachial plexus injury: an experimental study in rats. J Plast Reconstr Aesthet Surg 67:1282-1287.

Wang M, Xu W, Zheng M, Teng F, Xu J, Gu Y (2011) Phrenic nerve end-to-side neurotization in treating brachial plexus avulsion: an experimental study in rats. Ann Plast Surg 66:370-376.

Willand MP, Chiang CD, Zhang JJ, Kemp SW, Borschel GH, Gordon T (2015) Daily electrical muscle stimulation enhances functional recovery following nerve transection and repair in rats. Neurorehabil Neural Repair 29:690-700.

Zheng MX, Qiu YQ, Xu WD, Xu JG (2012a) Long-term observation of respiratory function after unilateral phrenic nerve and multiple intercostal nerve transfer for avulsed brachial plexus injury. Neurosurgery 70:796-801; discussion 801.

Zheng MX, Xu WD, Shen YD, Xu JG, Gu YD (2012b) Reconstruction of elbow flexion by end-to-side neurorrhaphy in phrenic nerve transfer. Plast Reconstr Surg 129:573e-575e.

(Copyedited by Yu J, Li CH, Qiu Y, Song LP, Zhao M)